

# Influence of the PZT Actuator Asymmetry on the LQR Control Parameters in the Active Reduction Vibrations of Beams

Romuald KURAS 

Laboratory of Acoustics, Department of Electrical and Computer Engineering Fundamentals, Rzeszow University of Technology, Wincentego Pola 2, 35-959 Rzeszow, Poland

**Corresponding author:** Romuald KURAS, email: r.kuras@prz.edu.pl

**Abstract** The paper deals with the active reduction of beam vibrations using piezoelectric transducers (PZT). The LQR parameters of the control of an asymmetric actuator (a-PZT) depending on the length of its arms were analysed. The results were compared to those of the symmetrical PZT (s-PZT), so far used as standard. The actuator is modeled with two bending moments or two pairs of forces. The design of the LQR controller also took into account the location of the PZT on the beam. The reduction efficiency can also be increased by using asymmetrical PZT. To obtain the vibration asymmetry of the beam, simply supported at both ends, an asymmetrically point mass was added. The LQR control was applied to an asymmetric actuator on the beam. Two-parameter optimization was used to find the optimal proportions of the a-PZT arms. For such a problem, the LQR control parameters were found, which ensure the highest efficiency of vibration reduction.

**Keywords:** beam, PZT, active vibration control, vibration reduction coefficient, effectiveness coefficient.

## 1. Introduction

Unwanted mechanical vibrations are a common phenomena in structures, buildings and vehicles. The vibrations are a threat to their integrity, functionality and, consequently, to human safety. Potential sources of vibration in objects can also influence the results of precise mechanisms or the data collection process. There are two main methods of vibration reduction: active and passive [1].

Active vibration control includes vibration isolation systems that dynamically respond to incoming vibrations. This means that they detect the vibration parameters and react to them. There are two main types of control systems for active vibration control: feedforward and feedback. The former is mainly used to compensate for regular, periodic vibrations, while the feedback system continuously detects and reacts to incoming vibrations. A typical feedback control system includes a sensing mechanism that reads vibrations in real time and an actuator that responds to these vibrations by adjusting isolation parameters to reduce incoming vibrations or by creating a signal that cancels them [1,2].

The piezoelectric actuator, as one of the links in the active vibration reduction system, is also an element in which one can find ways to increase the effectiveness of vibration reduction. Several studies have been conducted on the optimal location of the actuator, from which approximate approaches and approaches that use analytical premises can be enumerated. Among the approximate approaches, a large number are solutions using genetic algorithms or artificial intelligence. K.G. Aktas and I. Esen [3] investigated different positions of the PZT depending on the LQR control parameters. The resulting position of the actuator, which for the cantilever beam was in the beam clamped edge, confirms the correctness of the maximum bending moment criterion [4-6]. This article also links the optimal location of the PZT with the bending moment of the beam in the light of the LQR control parameters. This problem was solved semi-analytically for asymmetrical mode shapes in steady state vibrations [7]. E. Żołopa and A. Brański [5] proved that the LQ idea approach and the analytical approach are equivalent and lead to the same results.

The paper proposes a method for optimizing the position and asymmetry of the PZT arms. Such an actuator is an asymmetric actuator (a-PZT) and is a generalization of the standard symmetric PZT (s-PZT). Due to the fact that the reduction of vibrations is a dynamic process, the amplitude of vibrations in the open-loop control and the envelope of the closed-loop signal were chosen as optimization parameters.

## 2. Forced vibration of the beam

Differential equation for transverse vibration of beam under applied PZT with an attached point mass is given by

$$EI \frac{\partial^4 u}{\partial x^4} + (\rho A + \alpha_m) \frac{\partial^2 u}{\partial t^2} = f \tag{1}$$

where  $u$  is the transversal displacement of the beam, m;  $E$  is the Young's modulus, Pa;  $I = h_1 h_2^3 / 12$  is the second moment of area, m<sup>4</sup>;  $A = h_1 h_2$  is the area of cross-section, m<sup>2</sup>;  $h_1$  denotes thickness of the beam, m;  $h_2$  denotes width of the beam, m;  $\rho$  is the mass density, kg/m<sup>3</sup>;  $\alpha_m = m\delta(x - x_m)$  determines the mass value and location of the point mass ( $\alpha_m = 0$  for beam with no point mass), kg/m; and  $f$  represents an excitation from PZT, N.

A simply supported beam with an attached point mass is chosen as the research object [4]. The boundary conditions is given by  $u = 0$  and  $u'' = 0$  at both edges of the beam. Initial conditions are assumed to be zero. The presented problem is illustrated in Fig. 1.

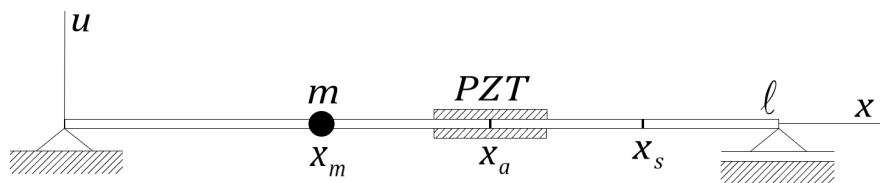


**Figure 1.** Simply supported beam with point mass at  $x_m$ , PZT at  $x_a$  and velocity sensor at  $x_s$ .

The following assumptions were made according to the Euler-Bernoulli theory [8]: the rotation of beam cross section is neglected (no shear deformation), neutral axis undergoes no extension. Using modal analysis, one can express the solution of the Eq. (1) as a linear combination of the normal modes

$$u(x, t) = \sum_{i=1}^{\infty} X_i(x) \eta_i(t), \tag{2}$$

where  $X_i(x)$  is the  $i^{th}$  mode shape of the beam and  $\eta_i(t)$  denotes the generalized displacement.

The mode shapes for a given problem may be found in [4,9]. Using Eq. (2), Eq. (1) can be expressed as

$$\sum_{i=1}^{\infty} \left[ EI \frac{\partial^4 X_i(x)}{\partial x^4} \eta_i(t) + (\rho A + \alpha_m) X_i(x) \ddot{\eta}_i(t) \right] = f(x, t). \tag{3}$$

Applying orthogonality condition  $\rho A \int_0^l X_i^2(x) dx = 1$  one can multiply by  $X_i$  and integrate from 0 to  $l$

$$\left( EI \int_0^l X_i(x) \frac{\partial^4 X_i(x)}{\partial x^4} dx \right) \eta_i(t) + \int_0^l (\rho A + m\delta(x - x_m)) X_i^2(x) dx \ddot{\eta}_i(t) = \int_0^l X_i(x) f(x, t) dx, \tag{4}$$

where  $\frac{\partial^4 X_i(x)}{\partial x^4} = \lambda_i^4 X_i(x)$ .

After some calculations Eq. (4) becomes

$$\frac{EI}{\rho A} \lambda_i^4 \eta_i(t) + \left( 1 + \frac{m X_i^2(x_m)}{\rho A} \right) \ddot{\eta}_i(t) = \int_0^l X_i(x) f(x, t) dx, \tag{5}$$

which simplifies Eq. (4) to the second order equation

$$\ddot{\eta}_i(t) + \frac{EI \lambda_i^4}{(\rho A + m X_i^2(x_m))} \eta_i(t) = \frac{\rho A}{(\rho A + m X_i^2(x_m))} \int_0^l X_i(x) f(x, t) dx. \tag{6}$$

### 3. Models of PZT actuators

Right hand side of the Eq. (1) represents the forces that make up the PZT. The actuator acts on the beam with two moments of the couple of forces that can be converted into two pairs of forces [4]. For the standard symmetrical PZT (see Fig. 2),

$$f(x, t) = f_n(t)[\delta(x - x_{1n}) - 2\delta(x - x_n) + \delta(x - x_{2n})], \tag{7}$$

where  $x_{1n} = x_n - L/2$ ,  $x_n$ ,  $x_{2n} = x_n + L/2$  are the location of the left edge, center and right edge of PZT, respectively,  $L$  is the length of PZT.

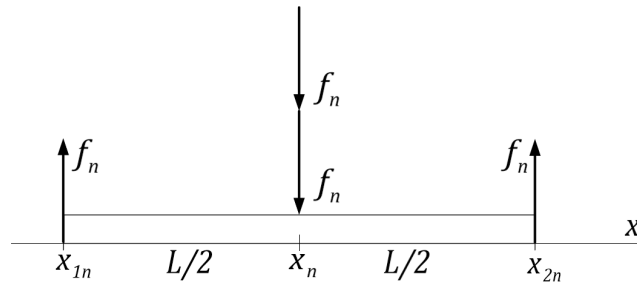


**Figure 2.** Model of the standard symmetrical PZT.

In the case of a-PZT (see Fig. 3), we assume that the moment of one couple of forces is equal to the moment of the second couple of forces, and their sum is equal to the moments from s-PZT:

$$f_n \frac{L}{2} + f_n \frac{L}{2} = f_1 \ell_1 + f_2 \ell_2; \quad f_1 \ell_1 = f_2 \ell_2 \tag{8}$$

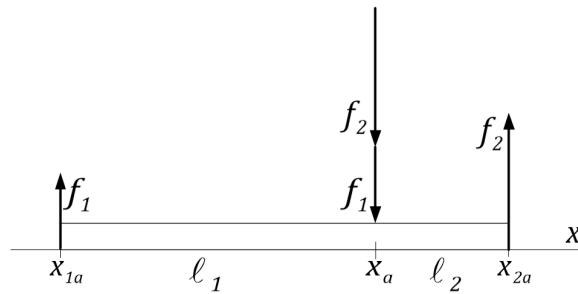


**Figure 3.** Model of the asymmetrical PZT.

Analogously to Eq. (7), we can derive RHS formula for the general case of PZT that taking into account different length of actuator arms, i.e. for a-PZT:

$$f(x, t) = f_1(t)\delta(x - x_{1a}) - (f_1(t) + f_2(t))\delta(x - x_a) + f_2(t)\delta(x - x_{2a}). \tag{9}$$

Substituting Eq. (8) into Eq. (9) one can obtain:

$$f(x, t) = \frac{1}{\ell_2} f_1(t)[\ell_2 \delta(x - x_{1a}) - (\ell_1 + \ell_2)\delta(x - x_a) + \ell_1 \delta(x - x_{2a})]. \tag{10}$$

And taking into account the integral on the RHS of Eq. (6), we can obtain a formula depending on the bending moment of the beam:

$$\int_0^\ell X_i(x) f(x, t) = \frac{1}{\ell_2} f_1(t)[\ell_2 X_i(x_{1a}) - (\ell_1 + \ell_2) X_i(x_a) + \ell_1 X_i(x_{2a})] = f_1(t) \frac{\ell_1^2}{\ell_2} X''(x_{1a}). \tag{11}$$

### 4. Transfer function and LQR design

#### 4.1. Transfer function with a-PZT

Based on Eqs. (6-10) we can get transfer function between a-PZT and non-collocated displacement sensor at  $x_s$  [8,10-11]:

$$G(s) = \sum_{i=1}^{\infty} \frac{k_a \frac{L}{2\ell_1\ell_2} [\ell_2 X_i(x_{1a}) - (\ell_1 + \ell_2) X_i(x_a) + \ell_1 X_i(x_{2a})] \cdot X_i(x_s)}{\mu_i (s^2 + \omega_i^2)}, \quad (12)$$

where  $k_a = \frac{\rho A}{(\rho A + m X_i^2(x_m))}$  and  $\mu_i$  is the generalized mass determined by  $\int_0^{\ell} \rho A X_i(x) X_j(x) dx = \mu_i \delta_{ij}$ .

#### 4.2. LQR controller design

First, the state space equations have been derived based on the equations of motion [8,11-12]:

$$\dot{\mathbf{x}} = \mathbf{A}\mathbf{x} + \mathbf{B}\mathbf{u} \quad (13)$$

$$\mathbf{y} = \mathbf{C}\mathbf{x}, \quad (14)$$

where  $\mathbf{x}$  is the state vector,  $\mathbf{y}$  is the output vector,  $\mathbf{u}$  is the input vector,  $\mathbf{A}$  denotes system matrix,  $\mathbf{B}$  denotes control matrix and  $\mathbf{C}$  is the output matrix.

Minimizing the cost function that is in the form of

$$J = \int_0^{\infty} (\mathbf{y}^T \mathbf{Q} \mathbf{y} + \mathbf{u}^T \mathbf{R} \mathbf{u}) dt \quad (15)$$

leads to obtain a control gain of the controller.  $\mathbf{Q}$  and  $\mathbf{R}$  are the power matrices. Input vector  $\mathbf{u}$  is defined as  $\mathbf{u} = -\mathbf{R}^{-1} \mathbf{B}^T \mathbf{P} \mathbf{x}$  where  $\mathbf{P}$  is the solution of the Riccati equation. The LQR controller has been designed for general case (a-PZT) that includes the special case of equal actuator arms (s-PZT):

$$\mathbf{A} = \begin{bmatrix} 0 & \omega_i \\ -\omega_i & 0 \end{bmatrix} \quad (16)$$

$$\mathbf{B} = \begin{bmatrix} 0 \\ \mu^{-1} \frac{L}{2\ell_1\ell_2} [\ell_2 X_i(x_{1a}) - (\ell_1 + \ell_2) X_i(x_a) + \ell_1 X_i(x_{2a})] \end{bmatrix} \quad (17)$$

$$\mathbf{C} = \begin{bmatrix} 0 \\ X_i(x_s) \end{bmatrix} \quad (18)$$

$$\mathbf{Q} = \mathbf{C}^T \mathbf{C}. \quad (19)$$

Non-collocated velocity sensor have been used in the LQR control algorithm simulation (see Eq. (18)).

### 5. Vibration reduction parameters

#### 5.1. System response under the PZT excitation

The first quantity that is a measure of the vibration reduction is the open-loop amplitude for different actuator arm lengths. Changing the location of the PZT changes the value of the beam deflection. Additionally, changing the ratio of a-PZT arms also affects the amplitude value. Thus, the problem is a two-parameter optimization in which the objective function (beam deflection amplitude) is maximized. If the a-PZT response reaches maximum, then such an actuator will be the most effective when applied to vibration reduction.

#### 5.2. Envelope of the signal

To find the optimal PZT parameters in the light of the LQR control, the closed-loop signal envelope was used. Figure 4 shows an exemplary signal and its envelope. Due to the symmetry, the upper envelope has been chosen and interpolated by an exponential model

$$y(t) = a e^{bt}. \quad (20)$$

A parameter directly related to vibration reduction in LQR control is the  $b$  coefficient of the envelope model, which determines how quickly the vibration will be vanished. The lowest value of  $b$  coefficient corresponds to the shortest time of vibration reduction. In this case, the objective function is simply the

$b$  parameter which is minimized (negative  $b$  values). Such a procedure leads to finding the actuator parameters that will vanish the vibrations most effectively.

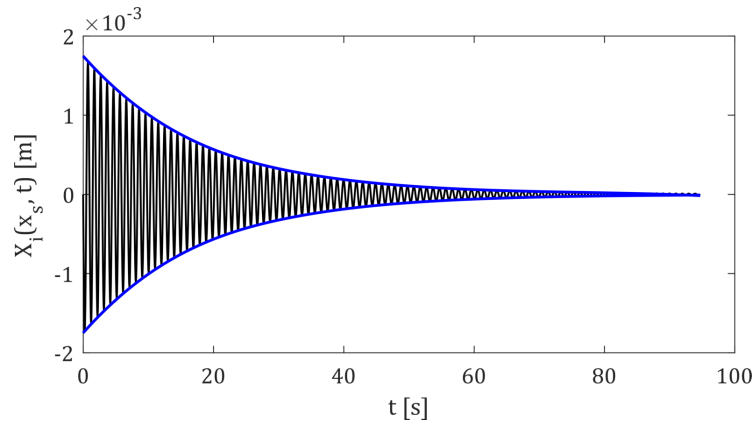


**Figure 4.** Sample closed-loop signal (black), envelope of the signal (blue).

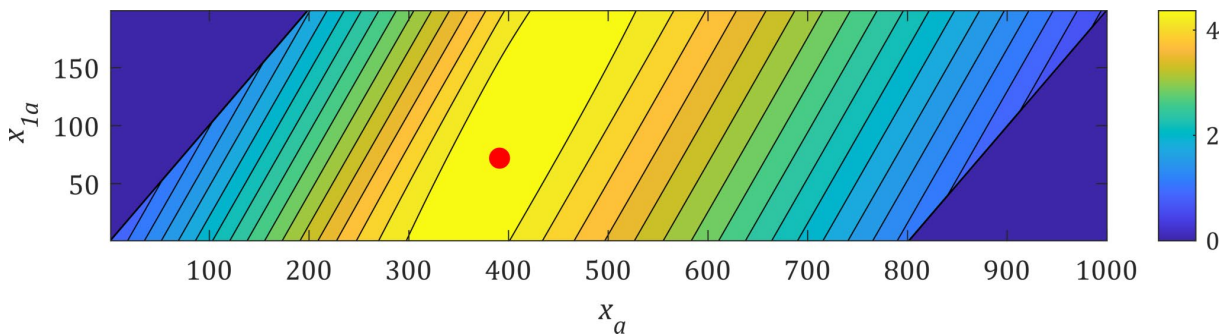
### 6. Numerical calculations

The calculations were made on the basis of the data assumed in Table 1. Next, 0.39 m for the first mode shape and 0.85 m for the second mode shape were assumed as the points of applied point mass  $x_m$ . The calculated natural frequencies in case  $x_m = 0.39$  m are as follows:  $\omega_1 = 6.4058$  rad/s,  $\omega_2 = 49.1687$  rad/s,  $\omega_3 = 117.8244$  rad/s,  $\omega_4 = 186.6459$  rad/s,  $\omega_5 = 358.2096$  rad/s,

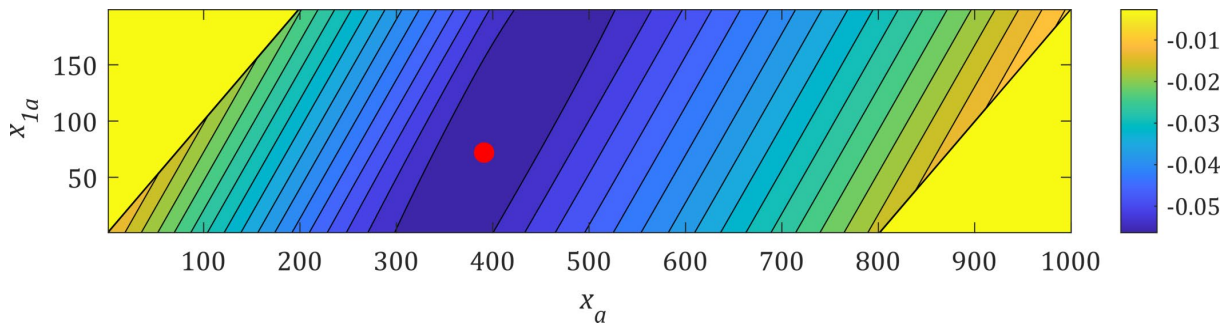
**Table 1.** Data used in calculations.

Quantity	Symbol	Unit	Value
Density	$\rho$	kg/m <sup>3</sup>	2700
Young's modulus	$E$	Pa	6.9e+10
Length of the beam	$\ell$	m	1
Thickness of the beam	$h_1$	m	0.001
Width of the beam	$h_2$	m	0.050
Weight of the point mass	$m$	kg	0.3
Length of PZT	$L$	m	0.2

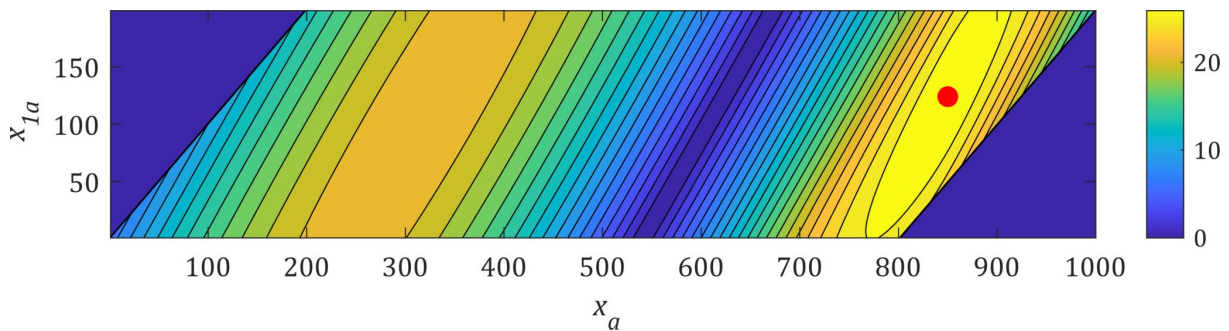
Figures 5-8 show the optimal a-PZT arm configuration (red dots). Comparative simulations were made for a beam with no point mass ( $\alpha_m = 0$ ), the results of which are presented in Fig. 9 (first mode shape). It is clearly shown that for symmetrical mode shapes the optimal PZT is symmetrical s-PZT. In contrast, while the mode shapes are asymmetrical ( $\alpha_m \neq 0$ ), a symmetrical actuator is not the best choice. In such cases, a-PZT is more effective and finding the optimal proportions of actuator arms is justified. Moreover, for a-PZT,  $x_a$  points are located at the absolute extremes of the beam bending moments (see Fig. 10).



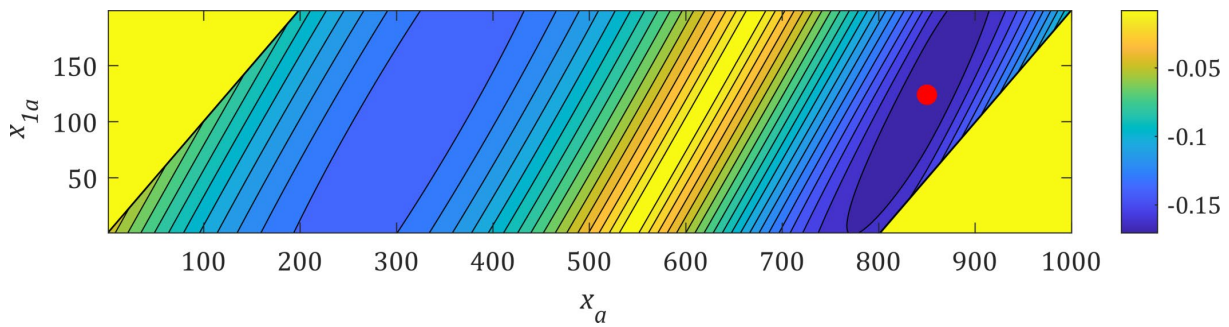
**Figure 5.** Distribution of the open-loop amplitude  $\times 10^{-6}$  at point  $x_s$  for the first mode shape.



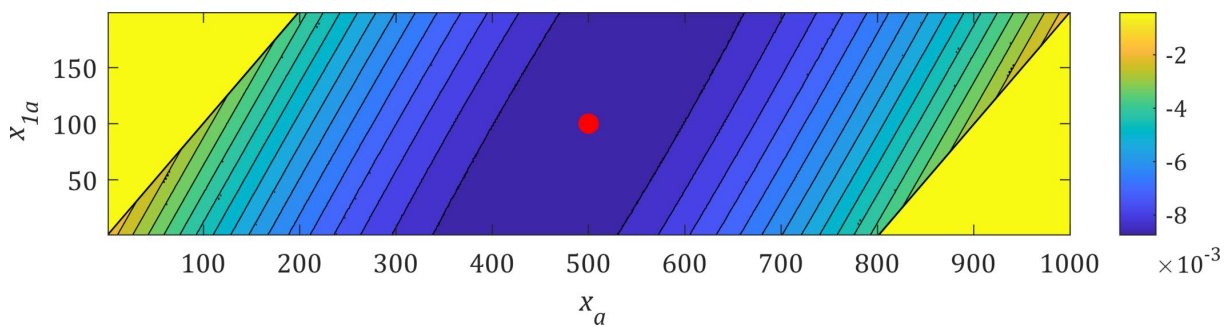
**Figure 6.** Distribution of the  $b$  coefficient for the first mode shape.



**Figure 7.** Distribution of the open-loop amplitude  $\times 10^{-6}$  at point  $x_s$  for the second mode shape.

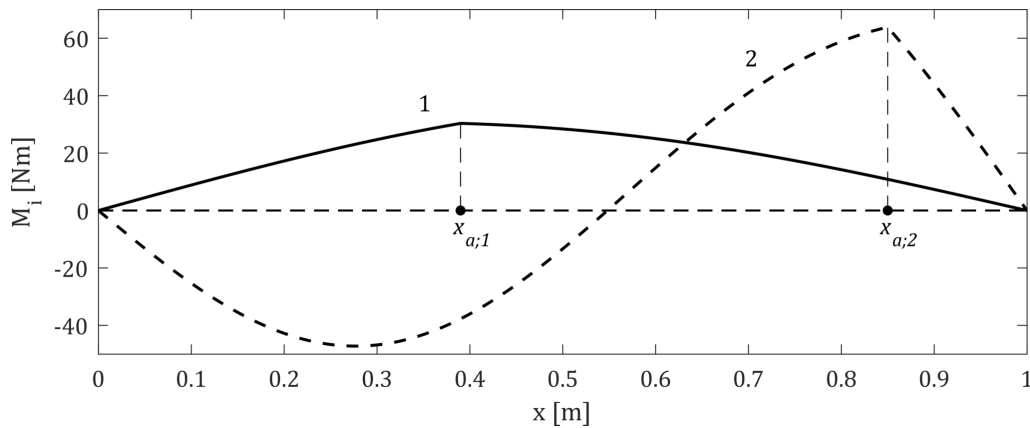


**Figure 8.** Distribution of the  $b$  coefficient for the second mode shape.



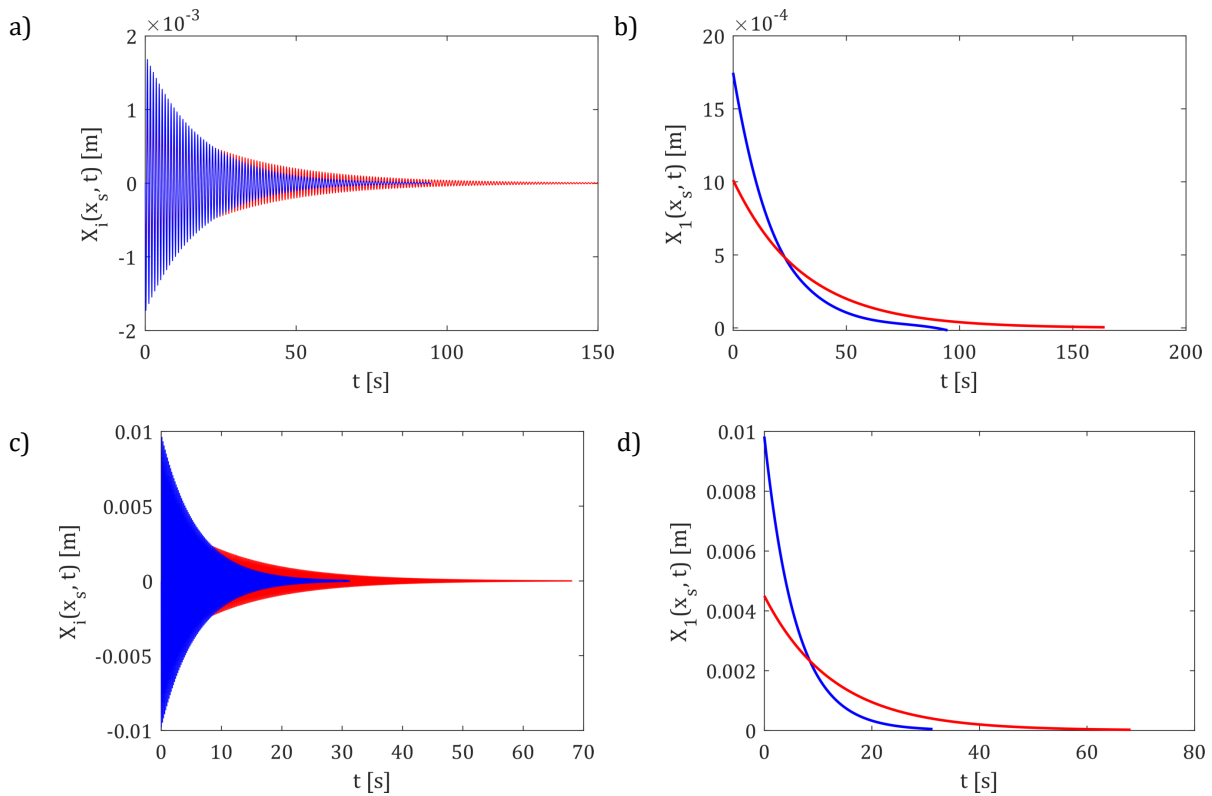
**Figure 9.** Distribution of the  $b$  coefficient for the first mode shape with no point mass.

Figure 11 shows the closed-loop simulation after applying the LQR controller. To show a clear difference in the plots and research methodology, the optimal a-PZT and arbitrarily s-PZT, that point  $x_n \neq x_a$ , were selected. A non-collocated velocity sensor was used as the sensor; for the 1<sup>st</sup> mode shape  $x_s = 0.5$  m and for the 2<sup>nd</sup> mode shape  $x_s = 0.3$  m.



**Figure 10.** The bending moments of the beam with attached point mass, first two mode shapes.

The parameters of the optimal actuator found in the light of LQR control are as follows: for the first mode shape  $\ell_1 = 0.072$  m,  $\ell_2 = 0.128$  m, for the second mode shape  $\ell_1 = 0.124$  m,  $\ell_2 = 0.076$  m. The point  $x_a$ , both for the 1<sup>st</sup> and 2<sup>nd</sup> mode shapes, is at the point of the point mass attached, i.e.  $x_{a;1} = 0.39$  m  $x_{a;2} = 0.85$  m.



**Figure 11.** Closed-loop simulations and their envelopes for a-PZT and s-PZT:

a) 1<sup>st</sup> mode shape, b) the envelope of the 1<sup>st</sup> mode shape, c) 2<sup>nd</sup> mode shape, d) the envelope of the 2<sup>nd</sup> mode shape.

### 7. Conclusions

The paper examines the problem of active vibration reduction of a simply supported beam with a point mass attached. The actuator was a piezoelectric transducer and its general model, i.e. a model that takes into account different lengths of the actuator arms. It has been shown that the most effective PZT is an individual feature of the mechanical system, because for each asymmetry of the beam mode shapes, there is an optimal a-PZT with a different configuration of the arms. Based on the calculations, the following conclusions can be drawn:

1. The a-PZT configuration on the basis of the beam vibration open-loop amplitude and the  $b$  coefficient of the assumed exponential model is consistent. Thus, these two parameters can be used to find the optimal a-PZT in the active reduction of beam vibration.
2. The criterion of the maximum bending moment in determining the optimal PZT solves the problem of actuator location and proportions of its arms.

The results presented in the article can be used to generalize the problem into a two-dimensional problem.

### Additional information

The author declare: no competing financial interests and that all material taken from other sources (including their own published works) is clearly cited and that appropriate permits are obtained.

### References

1. C.W. de Silva; *Vibration: Fundamentals and Practice*; CRC Press, Boca Raton, USA, 2000.
2. S.S. Rao; *Vibration of Continuous Systems*; John Wiley & Sons Inc., Hoboken, New Jersey, USA, 2007.
3. K.G. Aktas, I. Esen; *State-Space Modeling and Active Vibration Control of Smart Flexible Cantilever Beam with the Use of Finite Element Method*; *Engin. Technol. Appl. Sci. Res.* 2020, 10(6), 6549-6556. DOI: <https://doi.org/10.48084/etasr.3949>.
4. A. Brański; *An optimal distribution of actuators in active beam vibration – some aspects, theoretical considerations*; In: *Acoustic Waves*; M.G. Beghi Ed.; IntechOpen: Rijeka, Croatia, 2011, 397-418.
5. E. Żołąpa, A. Brański; *Comparison of Formulas Obtained for Analytical and LQ Idea Approaches to Determine the Optimal Actuator Location in Active Multimodal Beam Vibration Reduction*; *Arch. Acoust.* 2014, 39(4), 599-603. DOI: <https://doi.org/10.2478/aoa-2014-0064>.
6. E. Żołąpa, A. Brański; *Analytical Determination of Optimal Actuators Position for Single Mode Active Reduction of Fixed-free Beam Vibration Using the Linear Quadratic Problem Idea*; *Acta. Phys. Pol. A* 2014, 125. DOI: <https://doi.org/10.12693/APhysPolA.125.A-155>.
7. A. Brański, R. Kuras; *Asymmetrical PZT applied to active reduction of asymmetrically vibrating beam – semi-analytical solution*; *Arch. Acoust.* 2022, accepted.
8. A. Premount; *Vibration Control of Active Structures*, 3rd ed.; Springer, Berlin, Germany, 2011.
9. S. Kaliski; *Vibrations and Waves*; PWN, Warsaw, 1986.
10. S. Le; *Active vibration control of a flexible beam*, Master's Theses, San Jose State University, San Jose, USA 2009. DOI: <https://doi.org/10.31979/etd.r8xg-waar>.
11. Q. Mao, S. Pietrzko; *Control of Noise and Structural Vibration*; Springer, London, England 2013.
12. S.Q. Zhang, R. Schmidt; *LQR Control for Vibration Suppression of Piezoelectric Integrated Smart Structures*; *Proc. Appl. Math. Mech.* 2012, 12(1), 695-696. DOI: <https://www.doi.org/10.1002/pamm.201210336>.

© 2022 by the Authors. Licensee Poznan University of Technology (Poznan, Poland). This article is an open access article distributed under the terms and conditions of the Creative Commons Attribution (CC BY) license (<http://creativecommons.org/licenses/by/4.0/>).